ITERATIVE DEMODULATION OF ZERO-PADDED OFDM WITH MMSE EQUALIZATION USING A PRIORI INFORMATION

Stephan Pfletschinger

Centre Tecnològic de Telecomunicacions de Catalunya (CTTC)
Nexus I building, C/ Gran Capità 2-4, 08034 Barcelona, Spain
http://www.cttc.es/, email: stephan.pfletschinger@cttc.es

ABSTRACT

In this paper, we describe a novel scheme for iterative demapping, also known as turbo demodulation, of zero-padded (ZP) OFDM. Our scheme includes an MMSE equalizer which accepts *a priori* information delivered by an outer channel decoder. By enabling the equalizer to process independent reliability information about the encoded bits, the equalization stage can be included in the iterative decoding process, yielding superior performance when compared to iterative demapping. We derive an MMSE equalizer that accepts *a priori* information stemming from the outer decoder for several mappings and incorporate an additional rate-one inner code which removes the error floor, which is otherwise present in iterative demapping.

1. INTRODUCTION

Coded OFDM is one of the prime modulation schemes in modern wireless systems, which is due to its ability to efficiently deal with frequency-selective fading channels. A popular scheme, which is also applied in the prospering WLAN standards, is the combination of a convolutional code, an interleaver, a QAM symbol mapper and finally the FFT based OFDM modulation as depicted in Fig. 1. The combination of coding, interleaving and modulation is known as bit-interleaved coded modulation (BICM) [1] and since OFDM decomposes a frequency-selective broadband channel into parallel flat-fading channels, the principles of BICM and its decoding can be applied accordingly to the system in Fig. 1. A near-optimum method with moderate complexity for the decoding of BICM was first presented by ten Brink [2] and later adapted to OFDM by Muquet et al. [3]. This scheme is based on the turbo principle [4] and considers the convolutional code as outer code and the QAM mapping as inner "code". The idea to include the equalizer in the turbo iteration was presented by Tüchler et al. [5] in the context of single-carrier BICM.

In the transmitter in Fig. 1, the data bits c_k are encoded with a convolutional encoder and subsequently interleaved to yield the bit sequence $\mathbf{b} = [\mathbf{b}_0 \cdots \mathbf{b}_{N_\mathrm{C}-1}]$, where N_C is the number of subcarriers and the subsequences $\mathbf{b}_n = [b_{n1} \cdots b_{nQ}]$ contain Q bits belonging to one QAM symbol. The bits b_{nq} take on the values ± 1 and the vector $\mathbf{x}$ contains N_C QAM symbols belonging to one OFDM symbol:

$$\mathbf{x} = \begin{bmatrix} x_0 \\ \vdots \\ x_{N_\mathrm{C}-1} \end{bmatrix} = \begin{bmatrix} \mathrm{map}\,(\mathbf{b}_0) \\ \vdots \\ \mathrm{map}\,(\mathbf{b}_{N_\mathrm{C}-1}) \end{bmatrix}$$

with $x_n \in \mathcal{Q} = \{a_1, \ldots, a_{2Q}\}$. The QAM alphabet $\mathcal{Q}$ is assumed to be normalized and with zero mean, *i.e.* $\mathrm{E}[a_i] = 0$, $E_\mathrm{S} \triangleq \mathrm{E}[|a_i|^2] = 1$.

This work was partially funded by the Spanish Government grant HU2002-0032 and the Ministry of Universities, Research and Information Society, Generalitat de Catalunya.

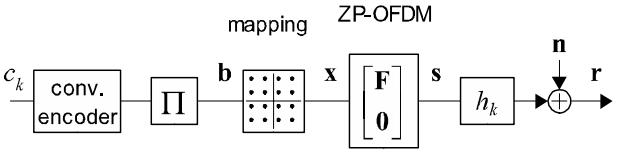

Figure 1: Transmitter with (outer) convolutional code, pseudo-random interleaver, QAM mapping and ZP-OFDM modulation.

The ZP-OFDM modulation can be conveniently described by

$$\mathbf{s} = \begin{bmatrix} \mathbf{F} \\ \mathbf{0}_{N_\mathrm{G} \times N_\mathrm{C}} \end{bmatrix} \mathbf{x}$$

where $\mathbf{F}$ with elements $F_{\nu\mu} = \exp(\frac{2\pi}{N_\mathrm{C}}\nu\mu)/\sqrt{N_\mathrm{C}}$; $\nu, \mu = 0, \ldots, N_\mathrm{C}-1$ is the *inverse* Fourier matrix and $\mathbf{0}_{n\times m}$ is the $n \times m$ all-zero matrix. The guard interval length is N_G, thus the length of the OFDM symbol $\mathbf{s}$ is $N_\mathrm{S} = N_\mathrm{C} + N_\mathrm{G}$. The channel impulse response h_k is assumed to have maximum length $N_\mathrm{G}+1$, thus intersymbol interference is prevented by the guard interval and the receiver input signal can be written as

$$\begin{aligned} \mathbf{r} &= \mathbf{H}\mathbf{s} + \mathbf{n} = [\mathbf{H_0}\ \mathbf{H}_{\mathrm{zp}}] \begin{bmatrix} \mathbf{F} \\ \mathbf{0}_{N_\mathrm{G} \times N_\mathrm{C}} \end{bmatrix} \mathbf{x} + \mathbf{n} \\ &= \mathbf{H}_0\mathbf{F}\mathbf{x} + \mathbf{n} \end{aligned}$$

where the noise correlation matrix is given by $\mathrm{E}[\mathbf{n}\mathbf{n}^{\mathcal{H}}] = N_0\mathbf{I}_{N_\mathrm{S}}$, where $(\cdot)^{\mathcal{H}}$ denotes conjugate transpose and $\mathbf{I}_n$ is the $n \times n$ identity matrix. The channel matrix $\mathbf{H}$ is the $N_\mathrm{S} \times N_\mathrm{S}$ lower triangular Toeplitz matrix with first column $[h_0 \cdots h_{N_\mathrm{G}}\, 0 \cdots 0]^\mathrm{T}$ and $\mathbf{H} = [\mathbf{H_0}\ \mathbf{H}_{\mathrm{zp}}]$ is its partition into the first N_C and the last N_G columns.

An iterative receiver structure for the ZP-OFDM system is depicted in Fig. 2. The MMSE (minimum mean square error) equalizer calculates an estimate of the QAM symbol x_n, from which the a posteriori probabilities (APP) $P[b_{nq} = \pm 1 | y_n]$ are calculated and output as extrinsic L-values E_1. The inner component "decoder" is hence formed by the MMSE equalizer and the APP calculation.

The extrinsic information from the inner decoder is deinterleaved to yield the input A_2 of the outer APP decoder, which implements the BCJR algorithm or one of its computationally more efficient approximations [6] to calculate the extrinsic information E_2 on the coded bits and the APP L-values $D_2^{(i)}$ for the information bits. After interleaving, the extrinsic information E_2 is fed to the inner "decoder" as a priori information A_1. This process is iterated several times and the estimates $\hat{c}_k$ on the data bits are finally obtained by hard decision of the L-values $D_2^{(i)}$.

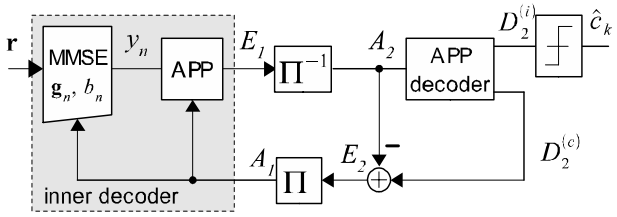

Figure 2: Iterative receiver for ZP-OFDM.

2. MMSE EQUALIZATION WITH A PRIORI INFORMATION

In the following we derive the inner decoder of the iterative receiver in Fig. 2. This derivation follows the lines of [5], but is adapted to ZP-OFDM and additionally considers non-Gray 8-PSK and 16-QAM mappings which provide better performance when used in conjunction with iterative decoding.

Reliability information about the bit b_{nq} is given by its a priori probability $P[b_{nq} = \pm 1]$ and is expressed as a priori L-value

$$A_{nq} \triangleq \ln \frac{P[b_{nq} = +1]}{P[b_{nq} = -1]}$$

In order to use this information in the MMSE equalizer, we first derive the mean and the variance of the QAM symbol x_n, given the a priori L-values $\mathbf{A}_n = [A_{n1} \cdots A_{nQ}]$. The mean $\bar{x}_n$ and variance v_n of x_n are given as

$$\begin{aligned} \bar{x}_n &\triangleq \mathrm{E}[x_n] = \sum\nolimits_{i=1}^{2^Q} a_i P[x_n = a_i] \\ v_n &\triangleq \mathrm{Cov}(x_n, x_n) = \left(\sum\nolimits_{i=1}^{2^Q} |a_i|^2 P[x_n = a_i] \right) - |\bar{x}_n|^2 \end{aligned}$$

The bits associated with the symbol a_i are written as $\hat{\mathbf{b}}_i = [\hat{b}_{i1} \cdots \hat{b}_{iQ}]$, *i.e.* $a_i = \mathrm{map}(\hat{\mathbf{b}}_i)$. Since the bits b_{nq} are independent due to the preceding interleaver, we can express the symbol probabilities as

$$\begin{aligned} P[x_n = a_i] &= P\left[\mathbf{b}_n = \hat{\mathbf{b}}_i\right] = \prod_{q=1}^{Q} P\left[b_{nq} = \hat{b}_{iq}\right] \\ &= \frac{1}{2^Q} \prod_{q=1}^{Q} \left(1 + \hat{b}_{iq} \tanh \frac{A_{nq}}{2}\right) \end{aligned}$$

For PSK mappings, the variance is given as

$$v_n = 1 - |\bar{x}_n|^2$$

With the abbreviations $\alpha_i \triangleq \tanh(A_{ni}/2)$; $a_{nm} \triangleq a_n a_m, \ldots$; $\iota \triangleq \sqrt{-1}$ we can write for mean and variance for the mappings given in Table 1 and Table 2:

QSPK gray: $\bar{x}_n = -(\alpha_2 + \iota\alpha_1)/\sqrt{2}$

QPSK Anti-Gray: $\bar{x}_n = (-\alpha_1 + \iota\alpha_{12})/\sqrt{2}$

8-PSK Gray:

$$\begin{aligned} \bar{x}_n = \tfrac{1}{4}\big(&(-1 - \iota(1+\sqrt{2}))\,\alpha_1 + (-1-\sqrt{2}+\iota)\,\alpha_2 \\ &+ (1-\sqrt{2}-\iota)\,\alpha_{13} + (1+\iota(1-\sqrt{2}))\,\alpha_{23}\big) \end{aligned}$$

8-PSK Anti-Gray:

$$\begin{aligned} \bar{x}_n = \tfrac{1}{4}\big(&(-1+\sqrt{2}-\iota)\,\alpha_2 + (-1+\iota(1-\sqrt{2}))\,\alpha_3 \\ &+ (1+\sqrt{2}+\iota)\,\alpha_{12} + (1-\iota(1+\sqrt{2}))\,\alpha_{13}\big) \end{aligned}$$

16-QAM SP:

$$\begin{aligned} \bar{x}_n &= \tfrac{1}{\sqrt{10}}(\alpha_{34} + 2\alpha_{124} + \iota 2\alpha_1 - \iota\alpha_3) \\ v_n &= 1 + \tfrac{2}{5}(-\alpha_{13} + \alpha_{123}) - |\bar{x}_n|^2 \end{aligned}$$

16-QAM Anti-Gray

$$\begin{aligned} \bar{x}_n &= \tfrac{1}{\sqrt{10}}(-\alpha_{124} - 2\alpha_{234} + \iota 2\alpha_{14} + \iota\alpha_{24}) \\ v_n &= 1 + \tfrac{2}{5}(\alpha_{12} + \alpha_{13}) - |\bar{x}_n|^2 \end{aligned}$$

16-QAM Bo1

$$\begin{aligned} \bar{x}_n = \; & \tfrac{1}{4\sqrt{10}}\{-\alpha_1 - \alpha_2 - 3\alpha_3 + \alpha_4 + 2\alpha_{12} - 2\alpha_{14} \\ & + 2\alpha_{23} + 2\alpha_{24} + \alpha_{123} + 3\alpha_{124} + 5\alpha_{134} - \alpha_{234} \\ & + 4\alpha_{1234} + \iota\cdot[\alpha_1 + \alpha_2 - 2\alpha_3 - 2\alpha_4 + \alpha_{13} - \alpha_{14} \\ & + \alpha_{23} + 3\alpha_{24} + 2\alpha_{123} + 2\alpha_{124} - 5\alpha_{134} - 5\alpha_{234}]\} \\ v_n = \; & 1 + \tfrac{1}{10}(\alpha_1 - \alpha_3 + \alpha_{12} + 2\alpha_{13} - \alpha_{14} + \alpha_{23} \\ & + \alpha_{34} - \alpha_{124} + 2\alpha_{134} - \alpha_{234} - 4\alpha_{1234}) - |\bar{x}_n|^2 \end{aligned}$$

Table 1: QPSK and 8-PSK symbol alphabets ($\iota = \sqrt{-1}$).

	8-PSK		QPSK	
i	Gray	Anti-Gray	Gray	Anti-Gray
1	1	1	$(1+\iota)/\sqrt{2}$	$(1+\iota)/\sqrt{2}$
2	$(1+\iota)/\sqrt{2}$	ι	$(-1+\iota)/\sqrt{2}$	$(1-\iota)/\sqrt{2}$
3	$(-1+\iota)/\sqrt{2}$	$-\iota$	$(1-\iota)/\sqrt{2}$	$(-1-\iota)/\sqrt{2}$
4	ι	-1	$(-1-\iota)/\sqrt{2}$	$(-1+\iota)/\sqrt{2}$
5	$(1-\iota)/\sqrt{2}$	$(-1+\iota)/\sqrt{2}$		
6	$-\iota$	$(-1-\iota)/\sqrt{2}$		
7	-1	$(1+\iota)/\sqrt{2}$		
8	$(-1-\iota)/\sqrt{2}$	$(1-\iota)/\sqrt{2}$		

Table 2: 16-QAM symbol alphabets.

i	SP	Anti-Gray	Bo1
1	$-1-\iota$	$3+3\iota$	$1+3\iota$
2	$1-\iota$	$-3-3\iota$	$3-3\iota$
3	$-3-3\iota$	$-1+3\iota$	$-1-3\iota$
4	$3-3\iota$	$1+3\iota$	$1+\iota$
5	$3-\iota$	$-3+\iota$	$-3+\iota$
6	$-3-\iota$	$3-\iota$	$3-\iota$
7	$1-3\iota$	$1+\iota$	$1-\iota$
8	$-1-3\iota$	$-1-\iota$	$-3-\iota$
9	$3+3\iota$	$1-\iota$	$3+3\iota$
10	$-3+3\iota$	$-1+\iota$	$-1-\iota$
11	$1+\iota$	$-3-\iota$	$-1+\iota$
12	$-1+\iota$	$3+\iota$	$-3-3\iota$
13	$-1+3\iota$	$-1-3\iota$	$1-3\iota$
14	$1+3\iota$	$1+3\iota$	$-1+3\iota$
15	$-3+\iota$	$3-3\iota$	$-3+3\iota$
16	$3+\iota$	$-3+3\iota$	$3-\iota$

The 16-QAM symbol alphabet "Bo1" was found by Boronka [7] by an extensive search as the mapping that reaches the lowest BER floor in iterative demapping. Unlike the other symbol alphabets, it contains almost no structure, which explains the lengthy expressions for $\bar{x}_n$ and v_n.

The correlation matrix of the receiver input and the correlation between receiver input and QAM symbol x_n are defined as

$$\begin{aligned} \mathbf{R_{rr}} &\triangleq \mathrm{Cov}(\mathbf{r}, \mathbf{r}) = \mathrm{E}[\mathbf{r}\mathbf{r}^{\mathcal{H}}] - \mathrm{E}[\mathbf{r}]\,\mathrm{E}[\mathbf{r}^{\mathcal{H}}] \\ \mathrm{Cov}(\mathbf{r}, x_n) &= \mathrm{E}[\mathbf{r}x_n^*] - \mathrm{E}[\mathbf{r}]\,\mathrm{E}[x_n^*] \end{aligned}$$

The equalizer outputs a linear estimate of the transmitted symbol x_n, given by

$$y_n = \mathbf{g}_n^{\mathcal{H}}\mathbf{r} + b_n \quad , n = 0, \ldots, N_{\mathrm{C}} - 1 \tag{1}$$

The solution that minimizes the mean square error (MSE)

$\mathrm{E}[|y_n - x_n|^2]$ can be calculated as [5]

$$\begin{aligned} \mathbf{g}_n &= \mathbf{R}_{\mathbf{rr}}^{-1} \operatorname{Cov}(\mathbf{r}, x_n) \\ b_n &= \bar{x}_n - \mathbf{g}_n^{\mathcal{H}} \mathrm{E}[\mathbf{r}] \end{aligned} \tag{2}$$

By defining $\mathbf{d}_n \triangleq \mathbf{H}_0\mathbf{F}\,[\mathbf{0}_{1\times n-1} \quad 1 \quad \mathbf{0}_{1\times N_\mathrm{C}-1}]^\mathrm{T}$ as the n-th column of $\mathbf{H}_0\mathbf{F}$, we can express the correlation vector and matrix as

$$\begin{aligned} \operatorname{Cov}(\mathbf{r}, x_n) &= v_n \mathbf{d}_n \\ \mathbf{R}_{\mathbf{rr}} &= \mathbf{H}_0\mathbf{F}\,\mathbf{R}_{\mathbf{xx}}\,\mathbf{F}^{\mathcal{H}}\mathbf{H}_0^{\mathcal{H}} + N_0\mathbf{I}_{N_\mathrm{S}} \\ \mathbf{R}_{\mathbf{xx}} &= \operatorname{diag}(v_0, v_1, \ldots, v_{N_\mathrm{C}-1}) \end{aligned} \tag{3}$$

where the last line is justified by the independence of the symbols x_n. With (2), we have determined a linear MMSE equalizer that takes into account *a priori* information given by the L-values on the bits b_{nq}. This MMSE equalizer can thus be included into the iterative decoding loop and can be considered part of the inner decoder. In iterative decoding schemes each component decoder should pass only extrinsic information to the other decoder[1] [4]. The estimate y_n according to (1),(2), however, depends on $\mathbf{A}_n$ via $\bar{x}_n$ and v_n. In order to pass extrinsic information only, we set $\mathbf{A}_n = \mathbf{0}_{1\times Q}$ for the calculation of y_n. This implies $\bar{x}_n = 0$ and $v_n = 1$, and we thus get from (2) with (3):

$$\begin{aligned} \mathbf{g}_n &= v_n \mathbf{f}_n, \quad \text{where} \quad \mathbf{f}_n \triangleq \mathbf{R}_{\mathbf{rr}}^{-1}\mathbf{d}_n \\ \mathbf{f}'_n &\triangleq \mathbf{g}_n|_{v_n=1} = \left(\mathbf{R}_{\mathbf{rr}} + (1-v_n)\mathbf{d}_n\mathbf{d}_n^{\mathcal{H}}\right)^{-1}\mathbf{d}_n \end{aligned} \tag{4}$$

With (4) and the matrix inversion lemma, which in this case results in a very simple expression [5], we can express $\mathbf{f}'_n$ as a scaled version of $\mathbf{f}_n$:

$$\mathbf{f}'_n = k_n \mathbf{f}_n \quad \text{with} \quad k_n = \frac{1}{1 + (1-v_n)\mathbf{f}_n^{\mathcal{H}}\mathbf{d}_n}$$

The estimate that contains a priori information from all other symbols is thus given by

$$y_n = k_n \mathbf{f}_n^{\mathcal{H}}(\mathbf{r} - \mathrm{E}[\mathbf{r}] + \bar{x}_n \mathbf{d}_n)$$

The second step in the inner component decoder consists of the calculation of the APP L-values which are defined as

$$\begin{aligned} D_{nq} &\triangleq L_D(b_{nq}|y_n) = \ln \frac{P[b_{nq}=+1|y_n]}{P[b_{nq}=-1|y_n]} \\ &= \ln \frac{\sum_{\hat{\mathbf{b}}_i \in \mathcal{B}_{+1}} p\left(y_n|\mathbf{b}_n = \hat{\mathbf{b}}_i\right) P\left[\mathbf{b}_n = \hat{\mathbf{b}}_i\right]}{\sum_{\hat{\mathbf{b}}_i \in \mathcal{B}_{-1}} p\left(y_n|\mathbf{b}_n = \hat{\mathbf{b}}_i\right) P\left[\mathbf{b}_n = \hat{\mathbf{b}}_i\right]} \end{aligned}$$

where $\mathcal{B}_{\pm 1} \triangleq \{\hat{\mathbf{b}}_i : \hat{b}_{iq} = \pm 1\}$. This expression can be written, making use of Bayes' theorem and the independence of the bits $b_{nq} \in \{-1, +1\}$, as $D_{nq} = A_{nq} + E_{nq}$ with the extrinsic information

$$E_{nq} = \ln \frac{\sum_{\hat{\mathbf{b}}_i \in \mathcal{B}_{+1}} p\left(y_n|\mathbf{b}_n = \hat{\mathbf{b}}_i\right) \exp\left(\frac{1}{2}\mathbf{A}_{n\bar{q}}\hat{\mathbf{b}}_{i\bar{q}}\right)}{\sum_{\hat{\mathbf{b}}_i \in \mathcal{B}_{-1}} p\left(y_n|\mathbf{b}_n = \hat{\mathbf{b}}_i\right) \exp\left(\frac{1}{2}\mathbf{A}_{n\bar{q}}\hat{\mathbf{b}}_{i\bar{q}}\right)}$$

The vector $\mathbf{A}_{n\bar{q}}$ is obtained from the vector $\mathbf{A}_n = [A_{n1} \cdots A_{nQ}]$ by deleting the element A_{nq}; the same holds for $\hat{\mathbf{b}}_{i\bar{q}}$. As in [5], we assume that the p.d.f. $p(y_n|\mathbf{b}_n = \hat{\mathbf{b}}_i) = p(y_n|x_n = a_i)$ is Gaussian:

$$p\left(y_n|\mathbf{b}_n = \hat{\mathbf{b}}_i\right) = \frac{1}{\pi\sigma_{ni}^2} \exp\left(-\frac{|y_n - \mu_{ni}|^2}{\sigma_{ni}^2}\right)$$

Then, the mean and the variance of y_n can be calculated as follows:

$$\begin{aligned} \mu_{ni} &\triangleq \mathrm{E}[y_n|x_n = a_i] \\ &= a_i \cdot k_n \mathbf{f}_n^{\mathcal{H}}\mathbf{d}_n \\ \sigma_{ni}^2 &= \operatorname{Cov}(y_n, y_n|x_n = a_i) \\ &= k_n^2\,\mathbf{f}_n^{\mathcal{H}}\mathbf{d}_n\left(1 - v_n\mathbf{d}_n^{\mathcal{H}}\mathbf{f}_n\right) \end{aligned}$$

where we made use of $\mathbf{d}_n = \mathbf{R}_{\mathbf{rr}}\mathbf{f}_n$, according to (4). Note that σ_{ni}^2 does not depend on i, and thus not on $\hat{\mathbf{b}}_i$, which allows us to write E_{nq} as

$$E_{nq} = \ln \frac{\sum_{\hat{\mathbf{b}}_i \in \mathcal{B}_{+1}} \exp\left(\rho_{ni} + \frac{1}{2}\mathbf{A}_{n\bar{q}}\hat{\mathbf{b}}_{i\bar{q}}\right)}{\sum_{\hat{\mathbf{b}}_i \in \mathcal{B}_{-1}} \exp\left(\rho_{ni} + \frac{1}{2}\mathbf{A}_{n\bar{q}}\hat{\mathbf{b}}_{i\bar{q}}\right)} \tag{5}$$

$$\rho_{ni} \triangleq -\frac{|y_n - \mu_{ni}|^2}{\sigma_{ni}^2} = -\frac{\left|\mathbf{f}_n^{\mathcal{H}}\mathbf{z}_n - a_i \cdot \mathbf{f}_n^{\mathcal{H}}\mathbf{d}_n\right|^2}{\mathbf{f}_n^{\mathcal{H}}\mathbf{d}_n - v_n\left|\mathbf{f}_n^{\mathcal{H}}\mathbf{d}_n\right|^2} \tag{6}$$

$$\mathbf{z}_n \triangleq \mathbf{r} - \mathrm{E}[\mathbf{r}] + \bar{x}_n\mathbf{d}_n$$

Summands in the nominator of (6) that do not depend on a_i cancel out in (5). We may thus replace ρ_{ni} by

$$\rho'_{ni} \triangleq \frac{2\,\mathrm{Re}\left\{a_i \cdot \mathbf{z}_n^{\mathcal{H}}\mathbf{f}_n\right\} - |a_i|^2\,\mathbf{f}_n^{\mathcal{H}}\mathbf{d}_n}{1 - v_n\mathbf{f}_n^{\mathcal{H}}\mathbf{d}_n} \tag{7}$$

where we used $\mathbf{f}_n^{\mathcal{H}}\mathbf{d}_n \in \mathbb{R}$. For PSK, the second summand in the nominator of (7) cancels out as well. The extrinsic information according to (5),(7) is thus passed via a de-interleaver to the outer decoder.

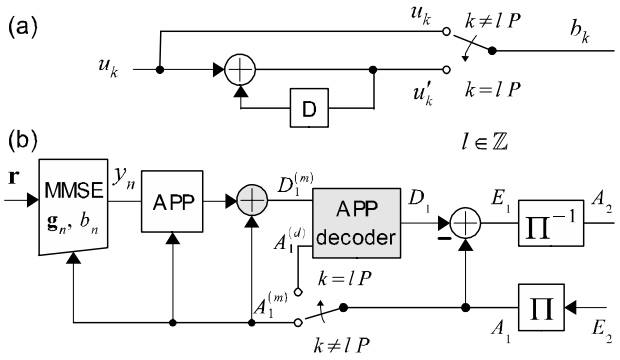

Figure 3: (a) Inner recursive rate-one convolutional code with code doping. (b) Changes in receiver structure to incorporate the corresponding inner decoder.

3. REMOVAL OF THE ERROR FLOOR

Iterative demapping systems for BICM typically suffer from an error floor which cannot be removed at the receiver side [2, 7, 8]. A possible countermeasure against this behavior is the insertion of an inner encoder according to Fig. 3*a* between the interleaver and the QAM mapper at the transmitter.

[1] Extrinsic information is information about one bit that can be gleaned from the knowledge of all other bits, considering the code constraints.

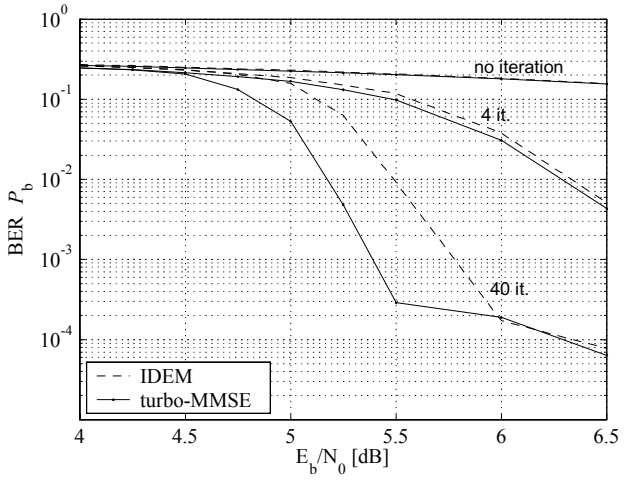

Figure 4: BER curves for ZP-OFDM. The reference receiver (IDEM) employs MMSE equalization with iterative demapping. The proposed receiver ("turbo MMSE") has an earlier turbo-cliff and a similar error floor behavior.

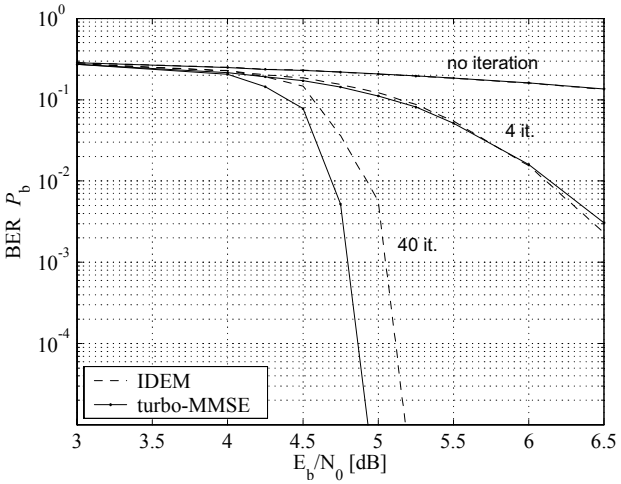

Figure 5: BER curves for ZP-OFDM with inner rate-1 code iterative demapping (IDEM) and turbo MMSE.

Only for every P-th bit, the input bit u_k is *substituted* by the differentially encoded bit u'_k:

$$b_k = \begin{cases} u_k & \mathrm{mod}_P(k) \neq 0 \\ u'_k & \mathrm{mod}_P(k) = 0 \end{cases}$$

In the following $P = 50$ is chosen. This process is called code doping and since it adds no redundancy it has no error correcting capabilities. Nevertheless, it introduces dependencies between adjacent bits and in conjunction with the corresponding decoder at the receiver side (Fig 3*b*) it removes the error floor. For a more detailed explanation based on transfer characteristics in the EXIT chart, we refer to [8].

At the receiver side, the corresponding APP decoder, which is a standard MAP decoder based on the BCJR algorithm, is inserted as illustrated in Fig. 3*b*.

4. SIMULATION RESULTS

Simulations have been performed with settings according to a WLAN environment, *i.e.* the number of subcarriers was chosen as $N_\mathrm{C} = 64$ and $N_\mathrm{G} = 16$ guard samples have been inserted. For each OFDM block, a different realization of the channel impulse response h_k according to model A of [9] has been drawn. For the outer code, the memory 2, recursive systematic convolutional code with polynomials $G_r = 07, G = 05$ has been used. The interleaver is pseudo-random and of length 51200 bits. The reference receiver employs MMSE equalization without a priori input and iterative demapping (IDEM) [2, 3] for the equalized symbols. Fig. 4 shows the BER curves for the transmitter in Fig. 1 and the described receiver vs. the reference receiver. The mapping in both systems was "16-QAM Bo1", which was found in [7] as the 16-QAM mapping with lowest error floor when decoded iteratively. As is well known, for iterative decoding, the otherwise optimal Gray mapping performs worst and is hence not considered in this paper. Fig. 4 shows a performance difference of nearly 0.5 dB in favor of the proposed equalization scheme and the expected error floor at $P_\mathrm{b} \approx 10^{-4}$.

The BER curves for the system with inner coding are depicted in Fig. 5. The inner code successfully removes the error floor and the coding gain in favor of the proposed system is reproduced for this case as well.

5. CONCLUSION

We presented a "turbo MMSE" receiver for ZP-OFDM which incorporates the equalization stage into the iterative decoding process and achieves a coding gain between 0.25 and 0.5 dB when compared to the reference receiver which employs a standard MMSE equalizer followed by an iterative demapping scheme. To our knowledge, this reference receiver is the best decoder for ZP-OFDM presented so far. It is also shown how this "turbo MMSE" equalizer fits into a BICM system with an inner code which removes the error floor without adding additional redundancy.

REFERENCES

[1] G. Caire, G. Taricco, E. Biglieri, "Bit-interleaved coded modulation," *IEEE Trans. Information Theory*, vol. 44, pp. 927-946, May 1998.

[2] S. ten Brink, J. Speidel, and R. H. Yan, "Iterative demapping and decoding for multilevel modulation," in *Proc. Globecom* 1998, Sydney, Australia, pp. 579-584.

[3] B. Muquet, M. de Courville, P. Duhamel, G. B. Giannakis, and P. Magniez, "Turbo demodulation of zero-padded OFDM transmissions," *IEEE Trans. Communications*, vol. 50, pp. 1725-1728, Nov. 2002.

[4] J. Hagenauer, "The turbo principle: Tutorial introduction and state of the art," in *Proc. Int. Symp. Turbo Codes*, Brest, France, Sept. 1997, pp. 1-11.

[5] M. Tüchler, A. C. Singer, and R. Koetter, "Minimum mean squared error equalization using a priori information," *IEEE Trans. Signal Processing*, vol. 50, pp. 673–682, Mar. 2002.

[6] P. Robertson, E. Villebrun, and P. Höher, "A comparison of optimal and sub-optimal MAP decoding algorithms operation in the log domain," in *Proc. ICC 1995*, Seattle, USA, June 1995, pp. 1009-1013.

[7] A. Boronka, J. Speidel, "A low complexity MIMO system based on BLAST and iterative anti-gray-demapping," in *Proc. PIMRC 2003*, Beijing, China, Sept. 2003.

[8] S. Pfletschinger and F. Sanzi, "Iterative demapping for ODFM with zero-padding or cyclic prefix," accepted at ICC 2004, Paris, France, June 2004.

[9] "Channel models for HIPERLAN/2 in different indoor scenarios," *ETSI*, Sophia-Antipolis, France, 1998.